Electronic Supplementary Material (ESI) for Journal of Materials Chemistry A.

Supporting Information

Oxygen-deficient 3D-ordered multistage porous interfacial catalysts with enhanced water oxidation performance

Xuemin Wang, Ming Liu, Haochen Yu, Hang Zhang, Sihao Yan, Cui Zhang and Shuangxi Liu

1. Related calculation formulas and equations

1.1 Electrocatalytic OER

Overpotential (η) was calculated by the following equation:

$$\eta\ (\mathrm{V}) = \mathrm{E_{RHE}} - 1.23\ \mathrm{V} \quad (1)$$

Tafel plots are showed with the linear portions at overpotential fitted to the Tafel equation:

$$\eta = b \log j + a \quad (2)$$

Where η is overpotential, j is the current density, b is the Tafel slope, and a is the exchange current density.

1.2 The ECSA and normalized current density are calculated as follows equation:

$$ECSA = \frac{C_{dl-samples}}{C_{dl-carbon\ paper}} \quad (3)$$

$$j_{ECSA-Normalized} = \frac{j}{ECSA} \quad (4)$$

Where C_{dl} is double layer capacitance, which was calculated by CV test under different sweep scan rates, and j is current density.

1.3 The values of mass activity (A g^{-1}) were calculated from the catalyst loading m (1 mg cm^{-2}) and the measured current density j (mA cm^{-2}) at η = 0.31 V.

$$\text{Mass activity} = j / m \quad (5)$$

1.4 The turnover frequency (TOF) was calculated according to the following formula:

$$\mathrm{TOF} = j \times \mathrm{A} / (4 \times \mathrm{F} \times m) \quad (6)$$

where j (mA cm^{-2}) is the current density at overpotential 310 mV, A is the surface area of the working electrode (1cm^2), F is the Faraday's constant (96485 C mol^{-1}), the

number 4 means that each molecule of O_2 has four electrons, and *m* is the number of moles of the catalysts on the electrodes (calculated from catalyst loading mass and the molecular weight of coating catalysts). All Co were assumed to be catalytically active whether they can get into the electrolyte or not. Therefore, the calculated TOF value represents the lower limit.

2. Instruments for characterization

The detailed microstructures were investigated with scanning electron microscopy (SEM; JEOL, JSM-7800F) and transmission electron microscopy (TEM, JEM-2800). Crystallographic information was collected by X-ray powder diffractometer (XRD; Rigaku MiniFlex600). The specific surface area and pore structure of the prepared sample was measured by a N_2 adsorption/desorption apparatus at 77 K (Micromeritics TriStar 3000). The surface composition and valence states were analyzed by X-ray photoelectron spectra (XPS; Thermo Scientific ESCALAB 250Xi).

3. Supporting Figures

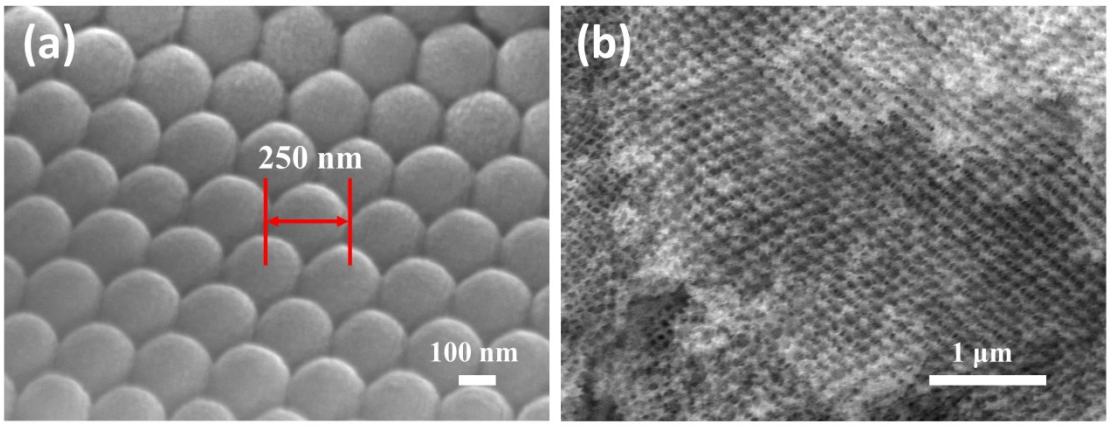

Figure S1. The SEM images of (a) 3D-PMMA template and (b) 3DOM-CC-10 electrocatalyst.

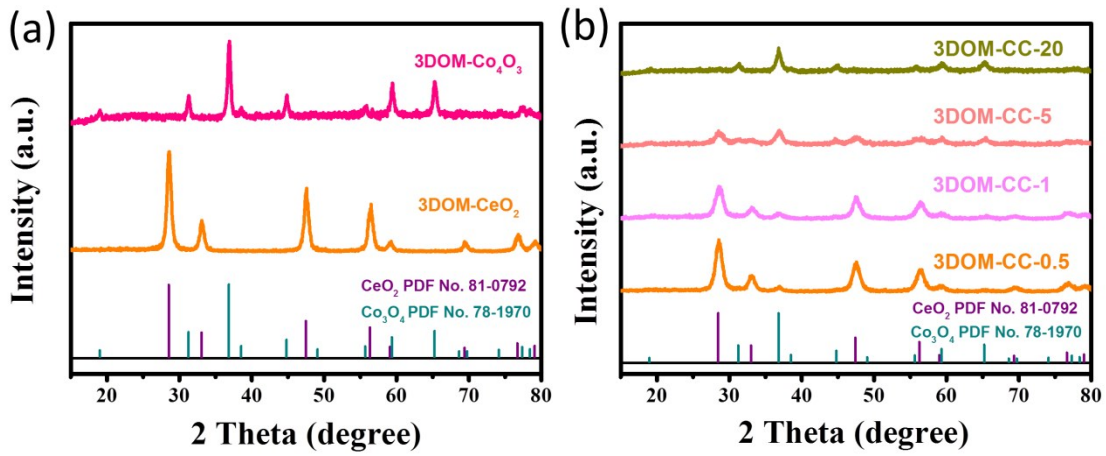

Figure S2. The XRD patterns of 3DOM-Co_3O_4, 3DOM-CeO_2 and 3DOM-CC-x.

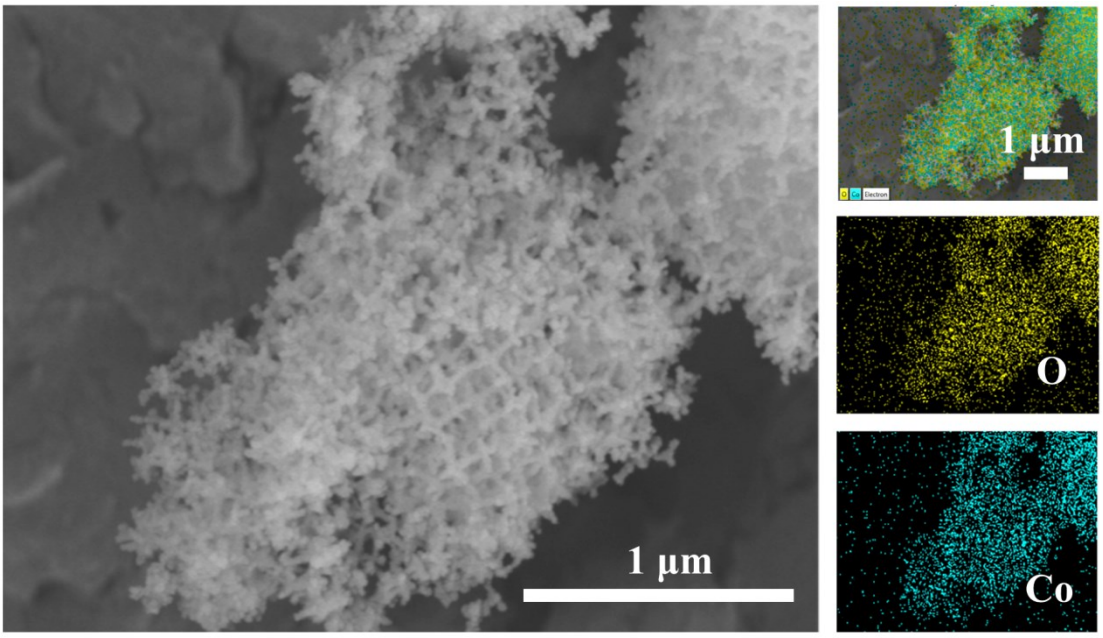

Figure S3. The SEM and corresponding mapping images of 3DOM-Co_3O_4.

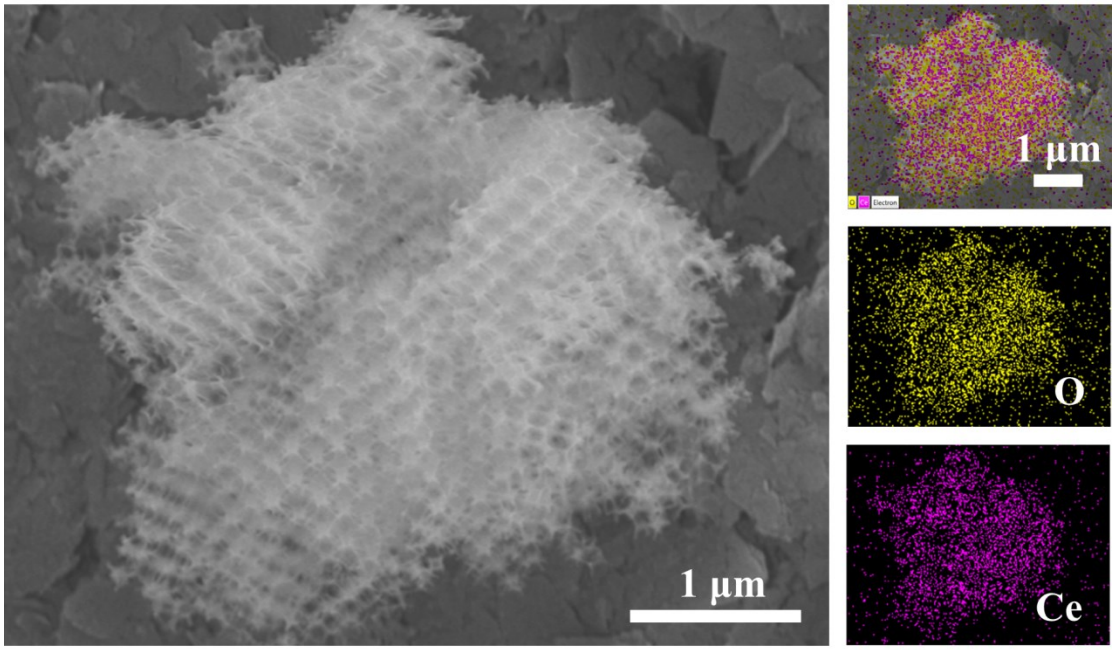

Figure S4. The SEM and corresponding mapping images of 3DOM-CeO_2

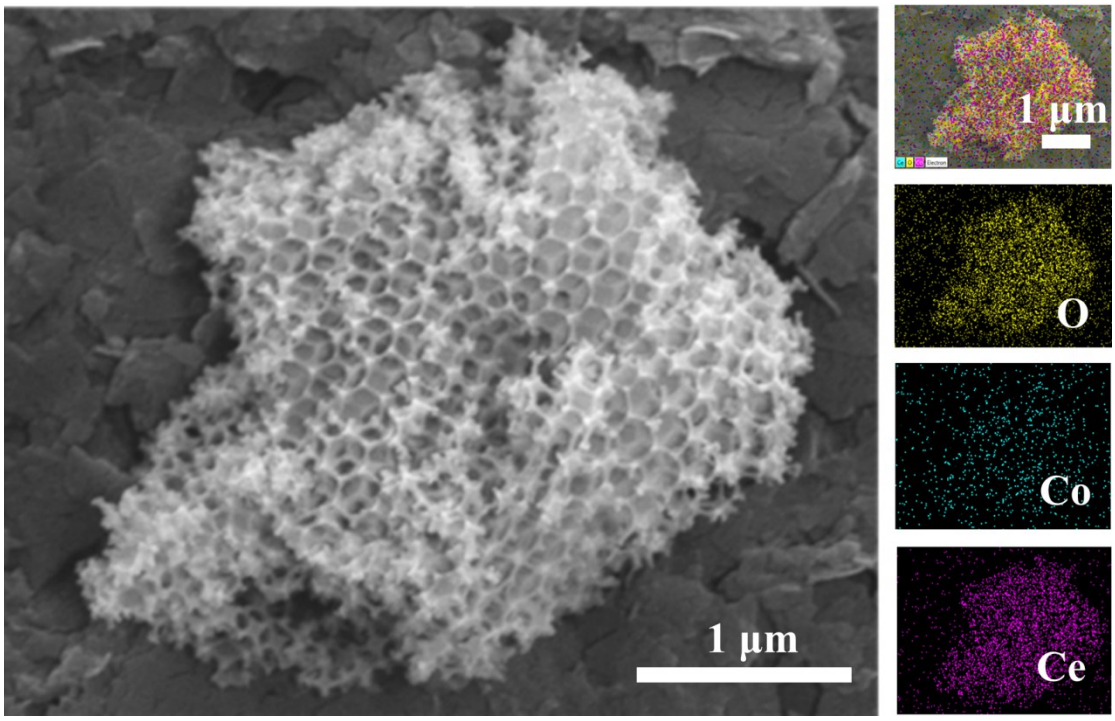

Figure S5. The SEM and corresponding mapping images and EDS of 3DOM-CC-20.

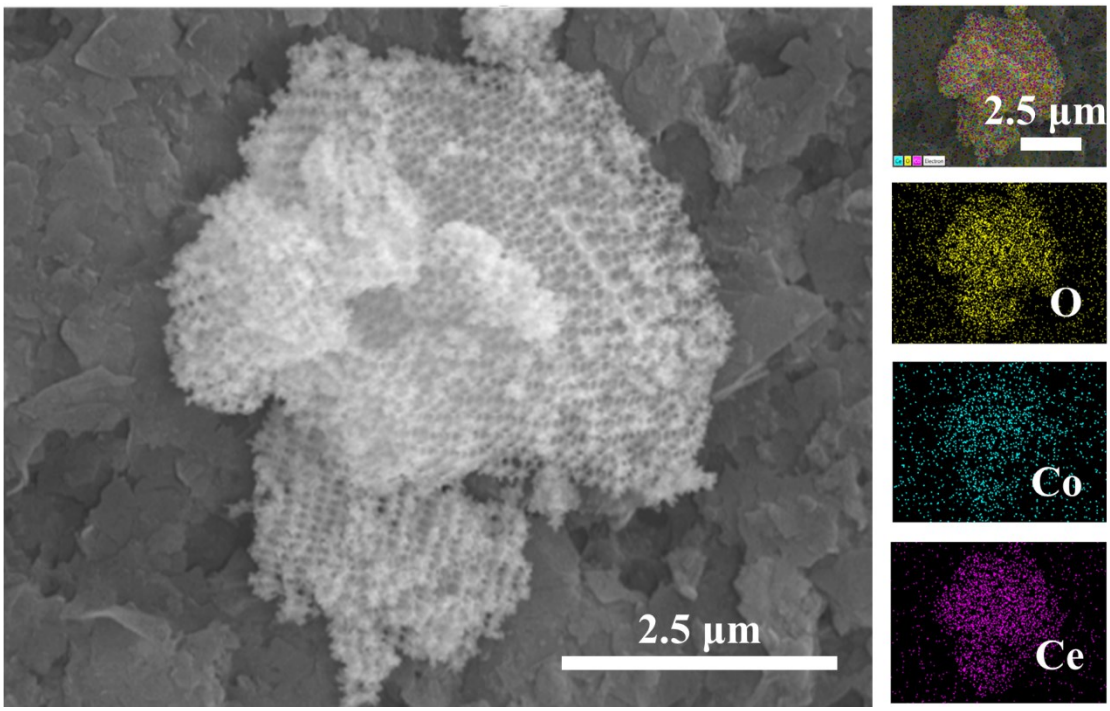

Figure S6. The SEM and corresponding mapping images and EDS of 3DOM-CC-5

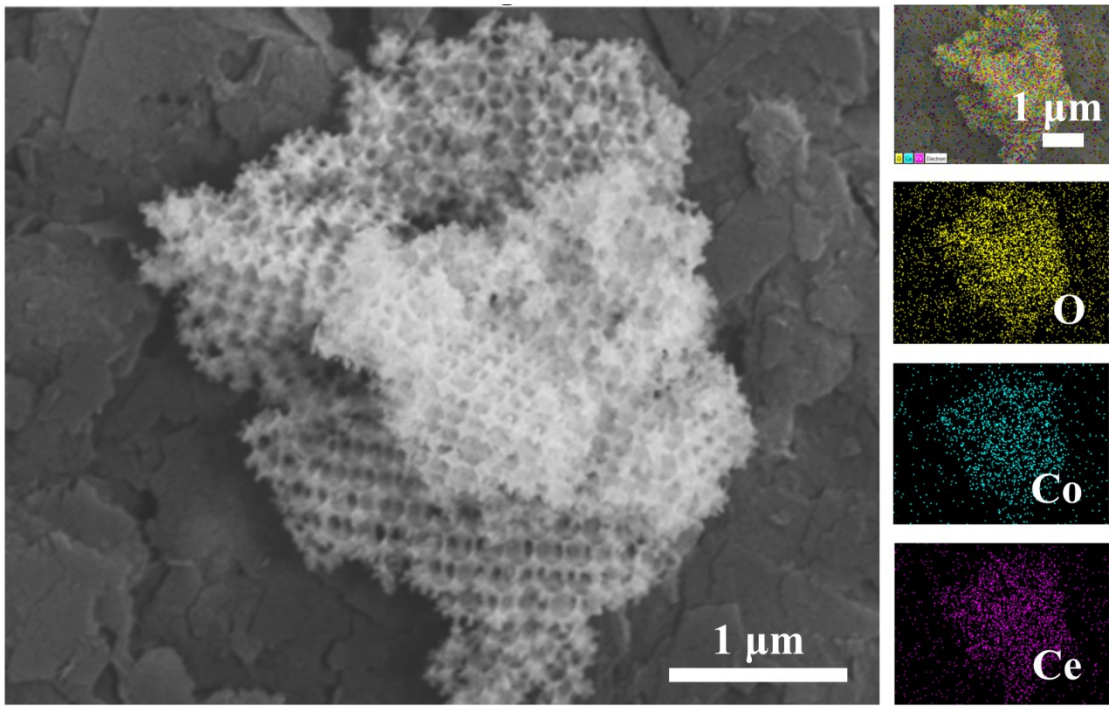

Figure S7. The SEM and corresponding mapping images and EDS of 3DOM-CC-1.

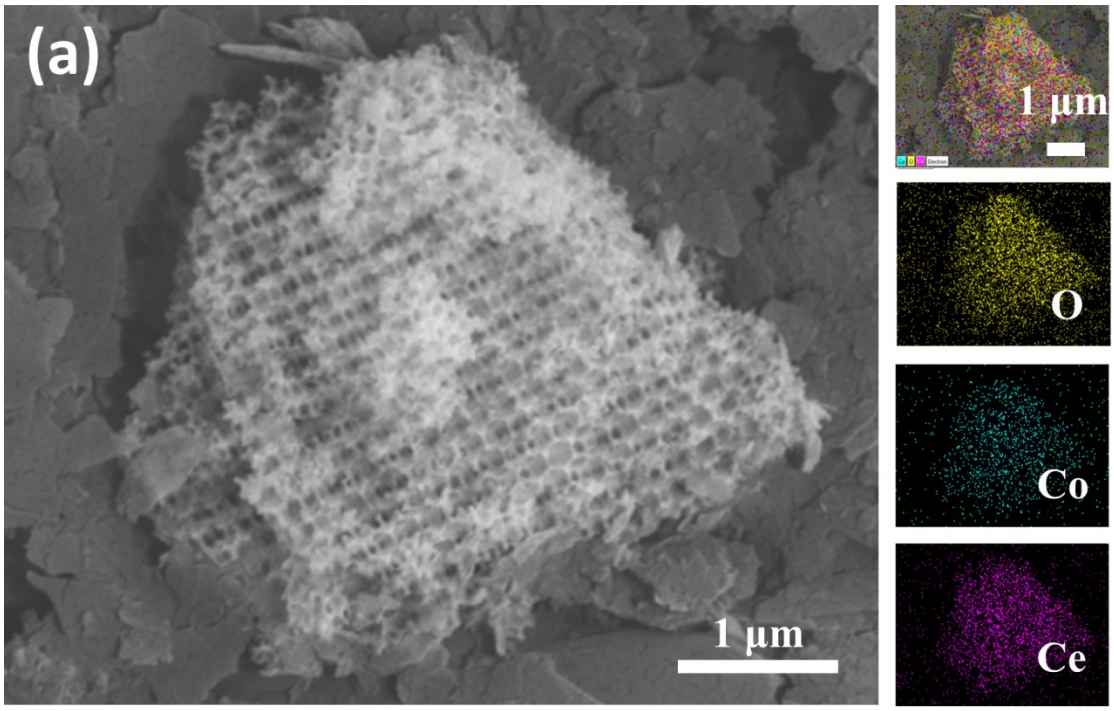

Figure S8. The SEM and corresponding mapping and images EDS of 3DOM-CC-0.5.

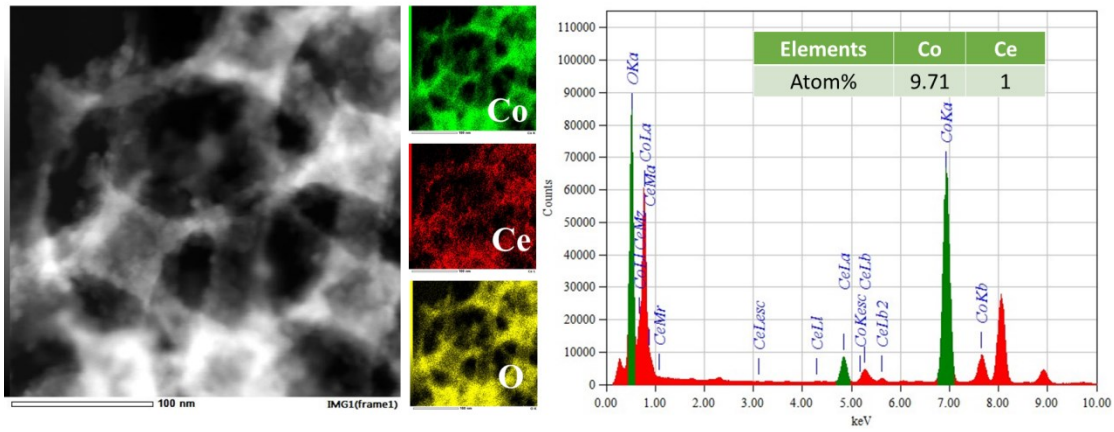

Figure S9. The TEM image, element mapping and EDX of (a) 3DOM-CC-10.

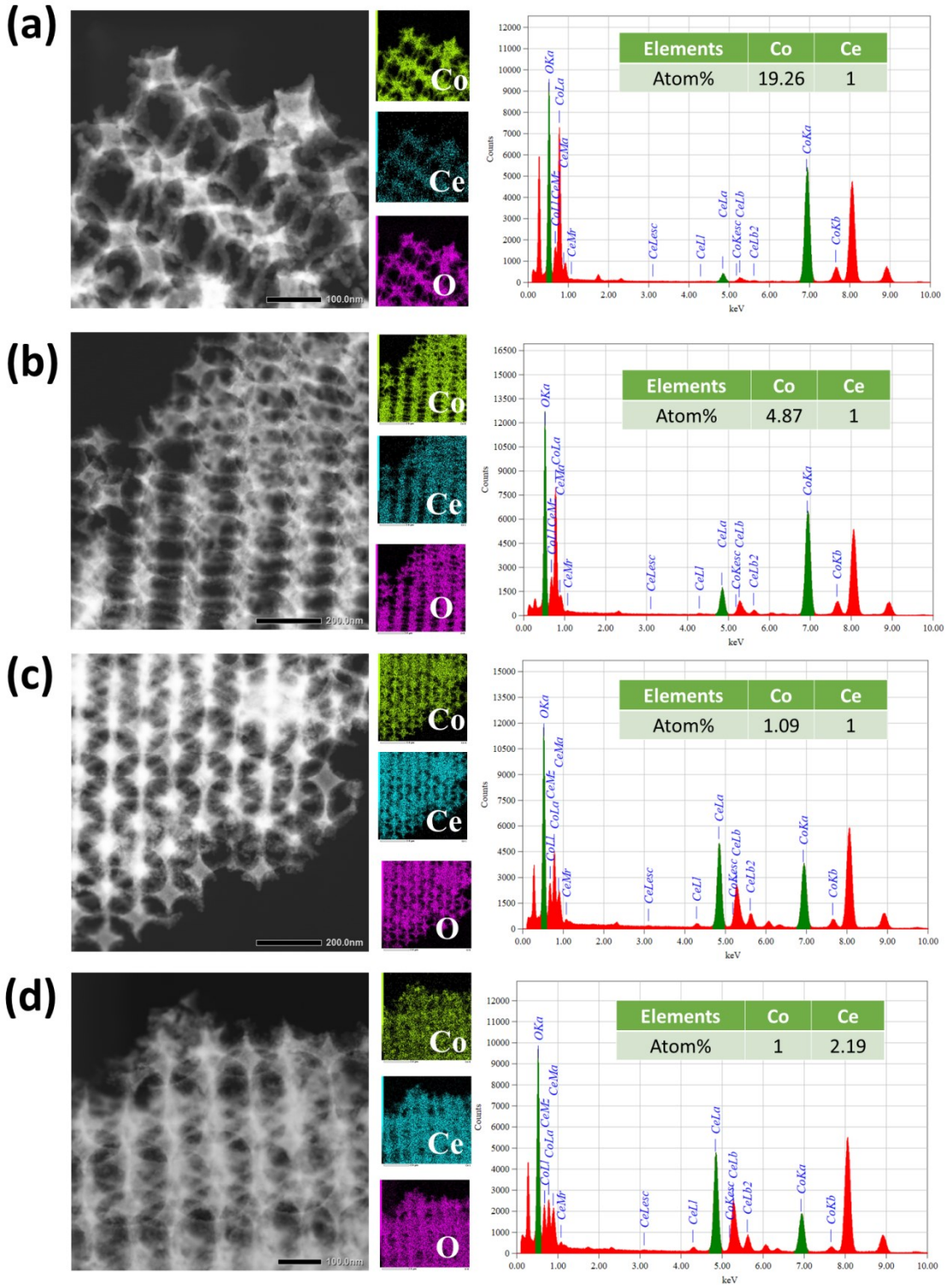

Figure S10. The TEM images, element mapping and EDX of (a) 3DOM-CC-20, (b) 3DOM-CC-5, (c) 3DOM-CC-1 and (d) 3DOM-CC-0.5.

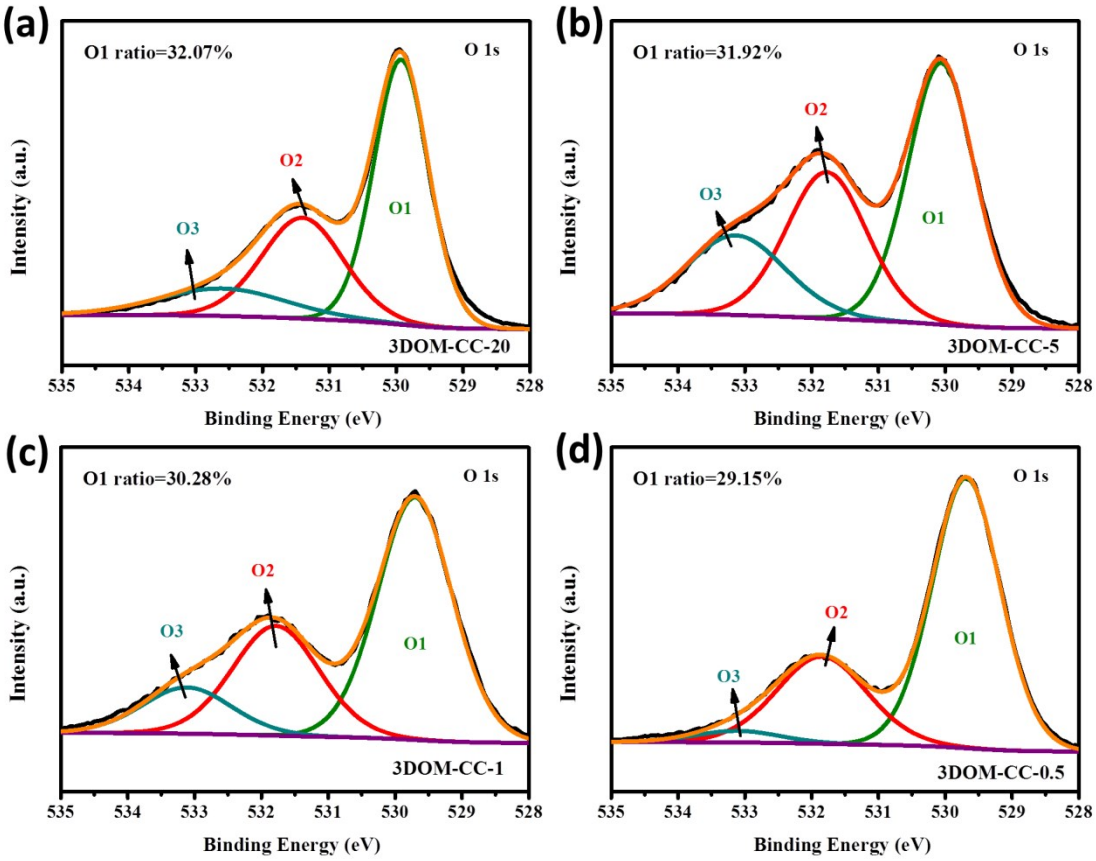

Figure S11. XPS O1s spectra of (a) 3DOM-CC-20, (b) 3DOM-CC-5, (c) 3DOM-CC-1 and (d) 3DOM-CC-0.5.

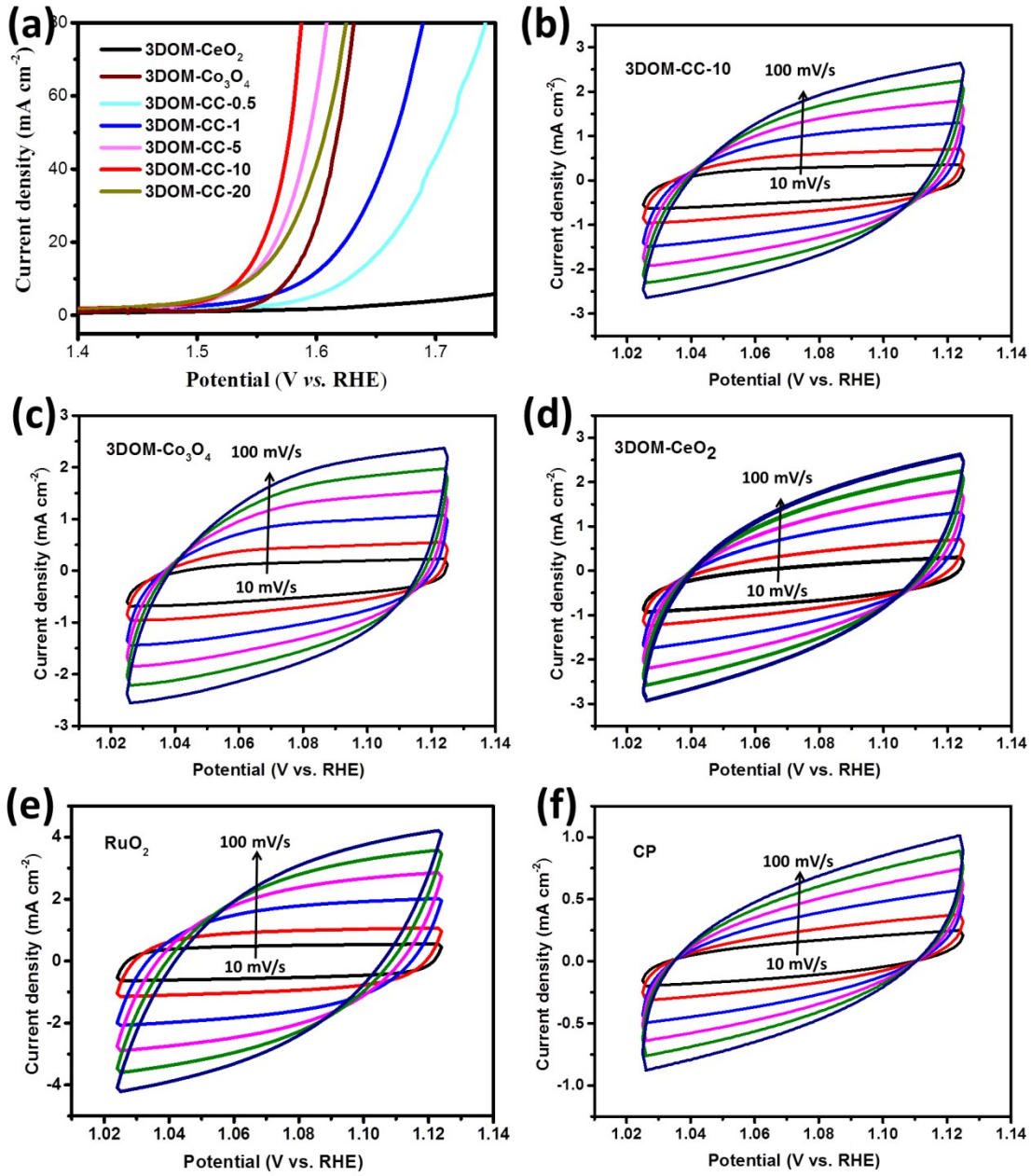

Figure S12. (a) LSV curves of 3DOM-Co_3O_4, 3DOM-CeO_2 and 3DOM-CC-x. (b) CV curves of 3DOM-CC-10, 3DOM-Co_3O_4, 3DOM-CeO_2, RuO_2 and CP.

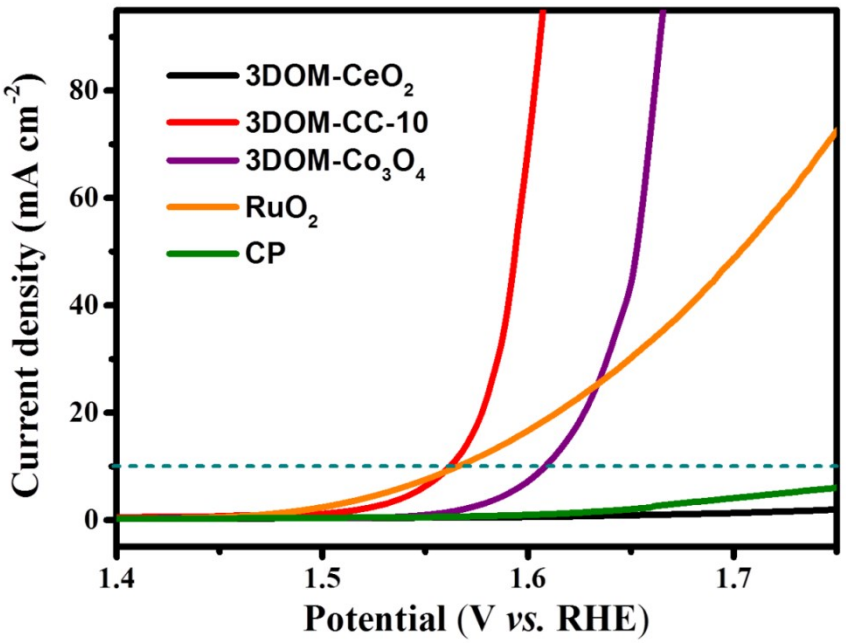

Figure S13. LSVs normalized by ECSA of different samples.

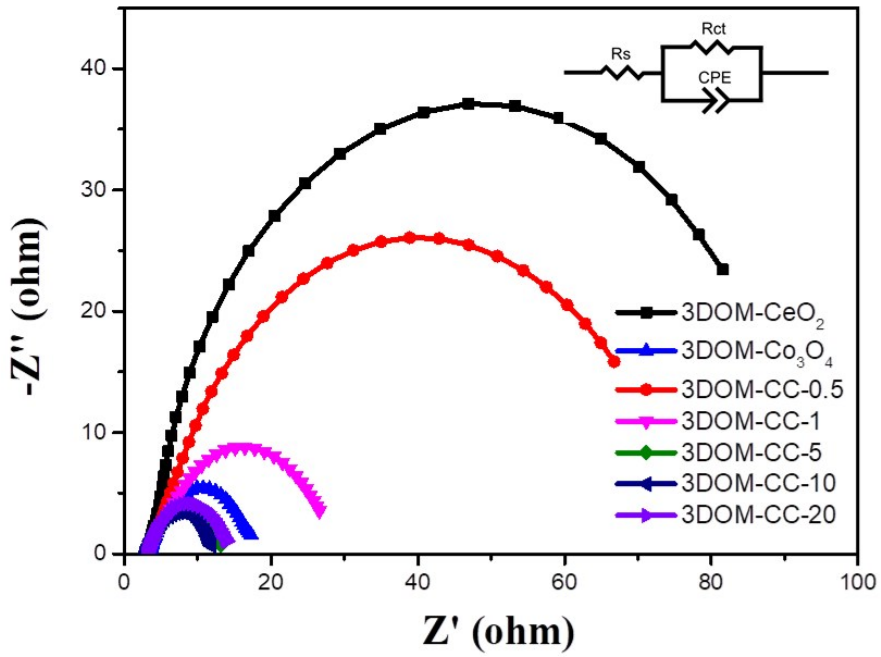

Figure S14. EIS Nyquist plots of samples.

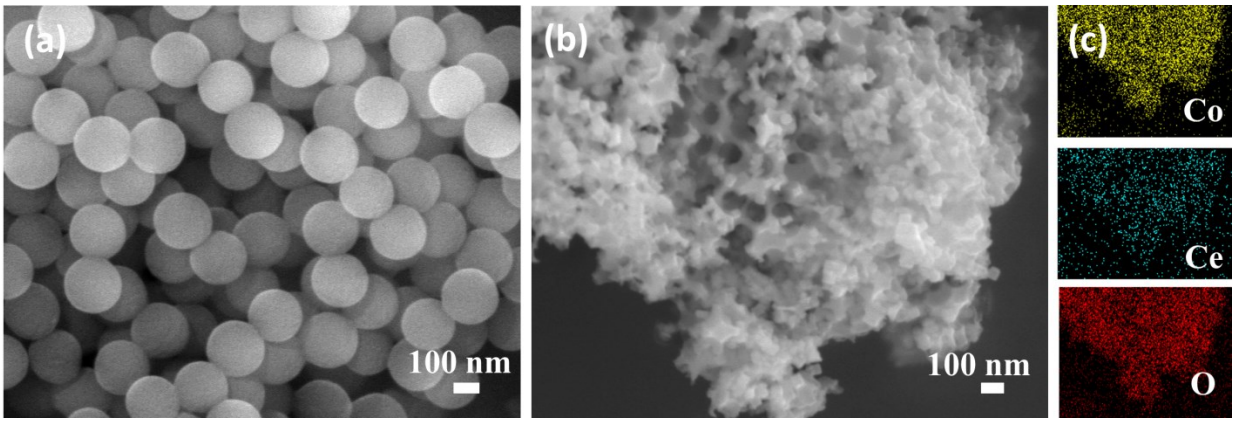

Figure S15. SEM images of Disorder-CC-10 (a) before and (b) after heat treatment.

(c) SEM elemental mapping images of Disorder-CC-10.

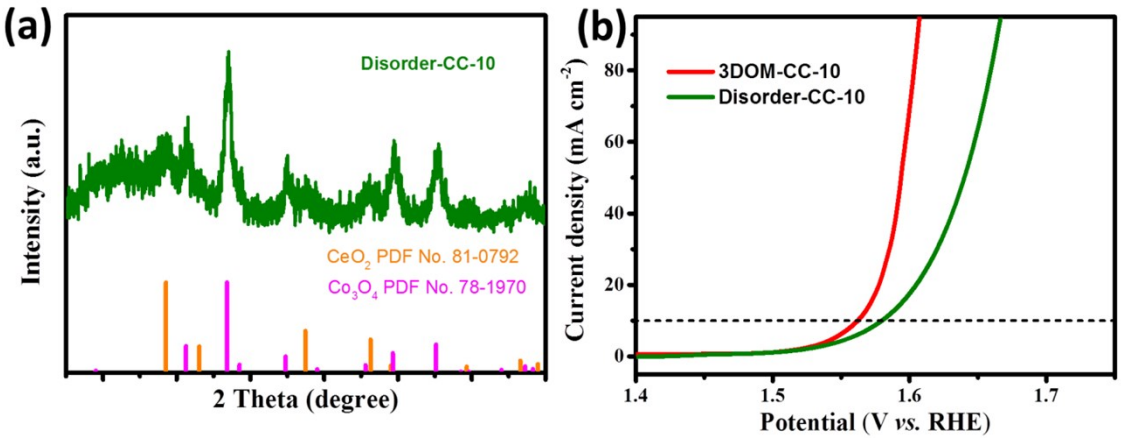

Figure S16. (a) XRD pattern and (b) LSV curves of Disorder-CC-10.

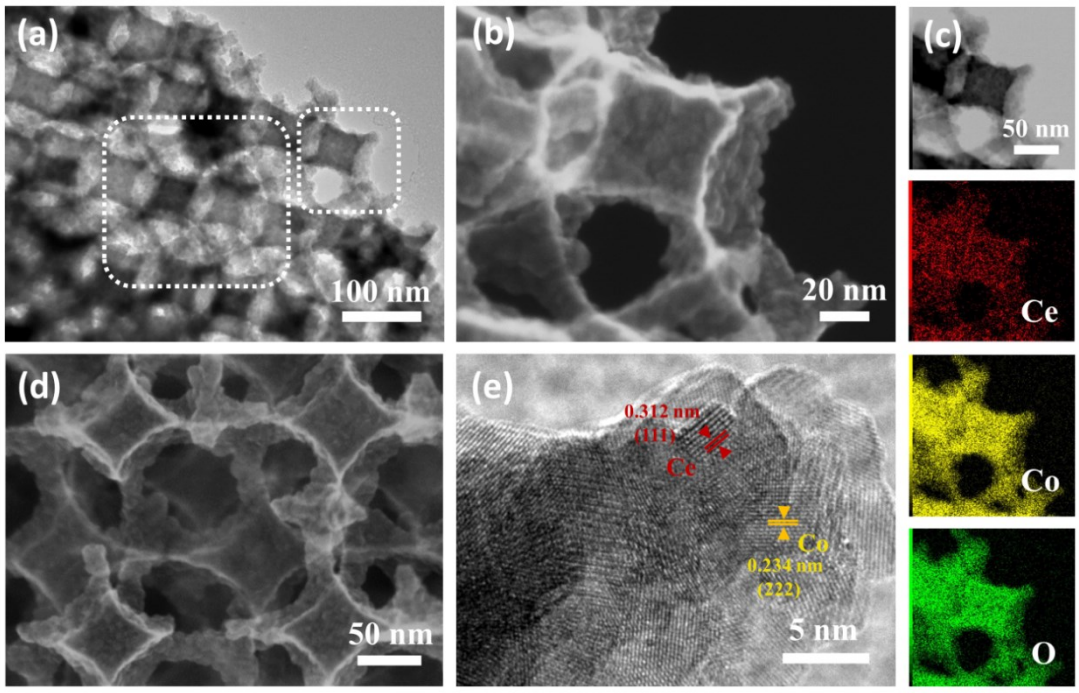

Figure S17. Morphology characterization of 3DOM-CC-10 after OER test. (a-b) the TEM images. (c) TEM elemental mapping images. (d) STEM images. (e) HRTEM image.

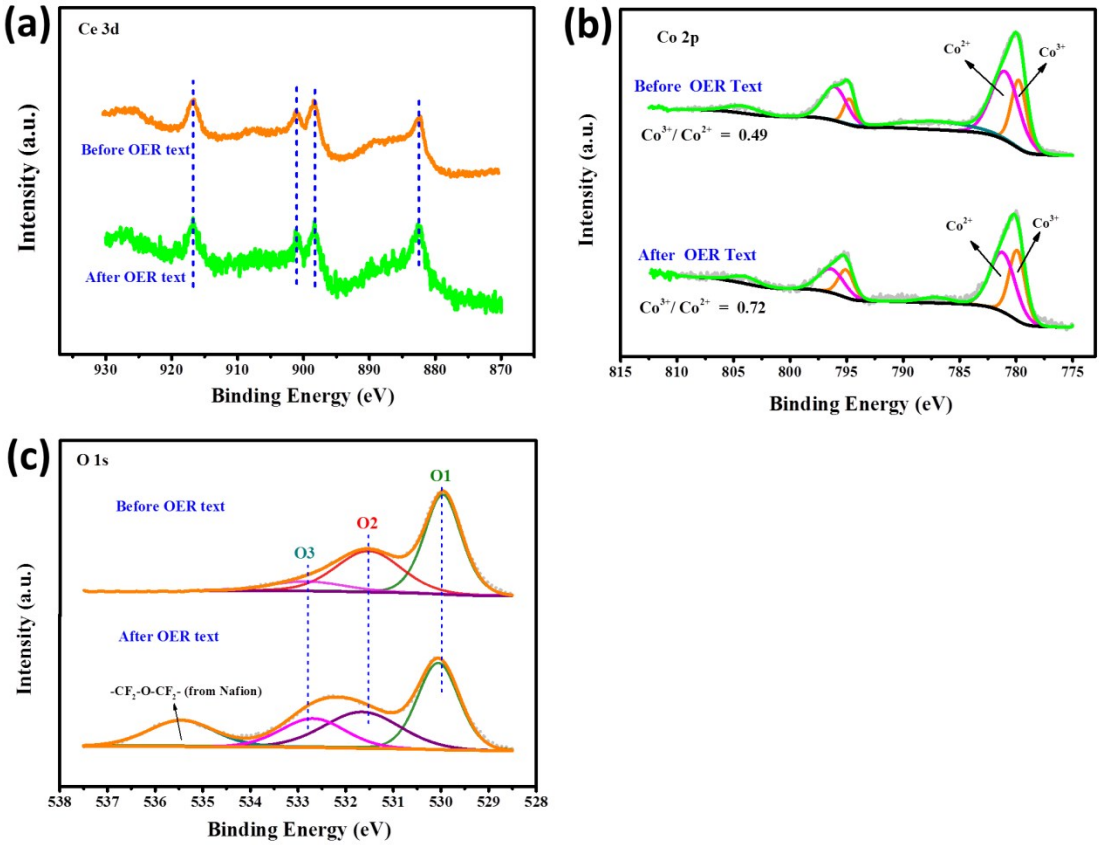

Figure S18. XPS (a) Ce 3d, (b) Co 2p and (c) O1s spectra of 3DOM-CC-10 before and after OER text.

Table S1. Summary of EDS results of samples with various Co/Ce ratios.

Sample	Added value of Co:Ce	Measured value of Ce:Co
3DOM-CC-20	20:1	19.26:1
3DOM-CC-10	10:1	9.71:1
3DOM-CC-5	5:1	4.87:1
3DOM-CC-1	1:1	1.09:1
3DOM-CC-0.5	1:2	1:2.19

Table S2. Comparison of the performance of 3DOM-CC-10 with similar catalysts reported in the literature

Catalysts	Overpotential / mV (10 mA cm^{-2})	Tafel slop ($mV\ dec^{-1}$)	Ref.
3DOM-CC-10	**298**	**49.5**	**This work**
CeO_x/CoO_x	313	66	ACS Catal., 2018, 8, 4257.
Ce-$MnCo_2O_4$-3%	390	125	ACS Sustain. Chem. Eng., 2018, 7, 1169.
h-$Co3O_4/CeO_2$@N-CNFs	310	85	ACS Sustainable Chem. Eng., 2019, 7, 17950.
Co-CeO_2/N-CNR	410	90	Appl. Catal. B-Environ., 2018, 237, 1148.
CeO_2/Co_3O_4	265	68.1	ACS Catal., 2019, 9, 6484.
CoO_x/FeO_x/CNTs	308	43	J. Mater. Chem. A, 2020, 8, 15140.
Co_3O_4@CoO	430	89	NPG Asia Mater., 2015, 6, 8106.
Ce-NiO	382	118.7	Adv. Funct. Mater., 2018, 28, 1706056
F-CoOOH/NF	270	54	Angew. Chem. Int. Ed., 2018, 57, 15471.
Plasma-Engraved Co_3O_4	300	68	Angew. Chem. Int. Ed., 2016, 55, 5277.
Co_3O_4 NW	320	72	Angew. Chem. Int. Ed., 2015, 54, 14710.
Ultrathin Co_3O_4	307	76	ACS Catal., 2018, 8, 1913.
CeOx/CoS	269	42	J. Mater. Chem. A, 2019, 7, 8284.
Co_3O_4/Co-Fe Oxide	297	61	Adv. Mater., 2018, 30, 1801211.
High-Index faceted Co_3O_4	318	66	ACS Appl. Mater. Inter., 2018, 10, 7079.

Fe-Co_3O_4	262	43	Adv. Mater., 2020, 32, 2002235.
$Co_3O_4/NiCo_2O_4$	340	88	J. Am. Chem. Soc. 2015, 137, 5590.